



Radiation crosslinked swellable ionic gels: equilibrium and kinetic studies of basic dye adsorption

Jhimli Paul Guin*, Y.K. Bhardwaj, Lalit Varshney

Radiation Technology Development Division, Bhabha Atomic Research Centre, Trombay, Mumbai 400 085, India, Tel. +91 022 25590175; Fax: +91 022 25505151; email: paul.jhimli@gmail.com (J. Paul Guin)

Received 27 March 2014; Accepted 11 November 2014

ABSTRACT

High-energy gamma radiation was employed to synthesize acrylic acid (AA)-based simple hydrogel adsorbent for environmental remediation of dye effluent. The adsorbent was tested for the aqueous solutions of two basic dyes, namely, Basic red 29 (BR 29) and Methylene blue (MB). The AA concentration of 20% (w/v) and absorbed dose of 30 kGy were optimized to synthesize AA hydrogel having good strength, and faster uptake kinetics for a wide range of dye concentration (10–5,000 mg/L). Equilibrium adsorption of both the dyes BR 29 and MB were better described by Langmuir adsorption. The equilibrium dye adsorption capacity onto AA hydrogel was found to be very high i.e. 1,123 mg/g (or 3.04 mmol/g) and 220 mg/g (or 0.68 mmol/g) for BR 29 and MB, respectively. The adsorption of BR 29 onto AA hydrogel followed the pseudo-first-order kinetics only in the initial time scale, whereas the adsorption of MB on AA hydrogel followed pseudo-second-order kinetics over the entire range of adsorption process. Desorption studies helped to elucidate the mechanism of dye adsorption and recycling of the spent adsorbent. The overall adsorption-desorption studies of these dyes on simple AA-based hydrogels are quite encouraging for more exploration.

Keywords: Gamma radiation; Acrylic acid; Adsorption; Basic red 29; Methylene blue

1. Introduction

The textile industries are vital to the economy of the developing countries. On the other hand, these countries face scarcity of freshwater which has grown to some extent due to the discharge of textile effluents into the ecosystem. The threats due to textile effluents come from the synthetic dye molecules, which are mostly bio-resistant and result in intense visible colour even at very low concentrations. The intense colour of the dye hinders sunlight penetration in water reducing

photosynthesis of phytons, aquatic plants, etc. and thus, threatens the whole ecosystem [1,2]. The heavy organic load from dye effluent causes a negative impact on the aquatic lives owing to the decrease in the dissolved oxygen concentration in the water stream [2]. The dyes in effluents are also source of associated aesthetic and toxicity problems. Therefore, an effective, efficient and economic method for the treatment of textile effluent is need of time.

The process of dyeing with reactive azo dyes under alkaline conditions renders the reactive group of dyes non-reusable. Thus, degradation is the ultimate fate of dyes for treatment of reactive dye

*Corresponding author.

effluents. Authors have been systematically putting efforts to develop an efficient advanced oxidation process for the mineralization of aqueous reactive azo dye solutions [3,4]. Unlike azo dyes, the residual basic dyes can be reused as they do not include any harsh alkaline digestion step during dyeing. Under this circumstances, adsorption–desorption might be considered as an useful technique for effectively lowering the concentration of dissolved dyes in the effluents [5,6]. Activated carbon is widely used for adsorbing dye molecules and other organic pollutants because of its high porosity and good surface area for sorption of organic compounds. However, the high cost and the drawbacks associated with handling of spent carbon limits its widespread application [7]. Hydrogels are polymeric materials that imbibe considerable amount of water within a polymeric network while keeping its three-dimensional stability [8]. They swell readily and adsorb heavy metal ions and dye molecules from water [9–14]. These are also used in agriculture, horticulture, personal care products and drug delivery [15].

Gamma radiation crosslinked hydrogels have several advantages over conventional crosslinked hydrogels [16]. The easy process control, absence of residual initiators, no requirement of multifunctional crosslinkers, no waste generation, relatively low running costs and sometimes more structural homogeneity of the network are major advantages of radiation crosslinked hydrogels. These make irradiation as the method of choice for synthesis of hydrogels. Radiation synthesized hydrogel adsorbents, both of synthetic and natural origin have been widely used for removal of dyes from aqueous medium in recent years. Natural polymeric adsorbents, such as chitin and chitosan [17], synthetic polymer-based hydrogels, such as acrylamide/itaconic acid hydrogel and [18] starch-based hydrogel [19] have been used for the removal of anionic and cationic dyes from aqueous solutions.

Basic red 29 (BR 29) and Methylene blue (MB) are the most frequently used basic dyes by acrylic fibre industries. Therefore, radiation crosslinked acrylic acid-based hydrogels (AA hydrogel) have been explored for removal of these model basic dyes from their aqueous solution in a wide concentration range (10–5,000 mg/L). Desorption studies were also performed to understand the mechanism of dye adsorption and recyclability of the spent adsorbent.

2. Experimental

2.1. Chemicals

AA, BR 29 and MB were purchased from Sigma-Aldrich and were used as such. The molecular struc-

tures of two dyes used in the study are shown in Fig. 1. All other chemicals used were of the highest purity and used without any pre-treatment.

2.2. Synthesis of hydrogels

Four different aqueous compositions of AA in range 5–50% (w/v) were irradiated using a ^{60}Co gamma chamber GC-5000 supplied by BRIT, India having a dose rate of 1.3 kGy h^{-1} as determined using Fricke dosimetry in the dose range of 5–40 kGy. The AA hydrogels were symmetrically cut into disc shapes and were swelled-dried for several cycles to remove trapped linear homopolymer or monomer and finally vacuum dried at 70°C .

2.3. Swelling studies of the hydrogels

The dynamic swelling of the hydrogels was carried out in distilled water at ambient temperature. The mass of the swollen gel was taken at different times till no further change in mass was noticed. The water uptake (W) of the hydrogels was determined by using Eq. (1):

$$W = \frac{(W_t - W_d)}{W_d} \quad (1)$$

where W_t is the mass of swollen hydrogel at time “ t ” and W_d is the mass of dry gel.

2.4. Adsorption of dyes

For equilibrium adsorption experiments, different concentrations of aqueous solutions of BR 29 and MB dyes were prepared covering a wide concentration range (10–5,000 mg/L). The hydrogels of known dried weight were immersed in known volume of the dye solutions for 24 h with continuous stirring, until equilibrium was reached. Then, dye solution was decanted and initial and equilibrium concentrations of dye solutions were determined by using UV-vis-2800

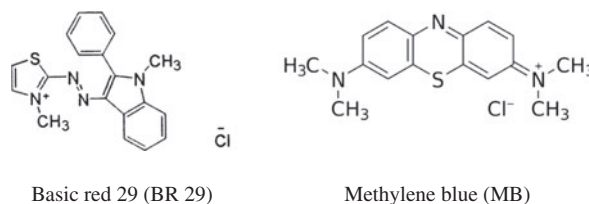


Fig. 1. The molecular structure of BR 29 and MB.

pectrophotometer at $\lambda_{\max} = 508$ nm and 661 nm for BR 29 and MB, respectively, using a pre-calibrated curve of absorbance vs. concentrations. The amount of dye uptake (in mg) by unit mass (in g) of the hydrogel (q_e in mg/g) was calculated using Eq. (2):

$$q_e = \frac{(C_0V_0 - C_eV)}{W_d} \quad (2)$$

where C_0 and C_e are the initial and equilibrium concentrations of dye solution (in mg dm^{-3}), while V_0 and V are volumes (in dm^3) of the initial and equilibrium dye solutions and W_d is the mass (in g) of the dry hydrogel used for the experiment. The uptake of dye i.e. the % removal of dye by the hydrogel was determined using Eq. (3):

$$\% \text{ Removal} = \frac{(C_0 - C_e)}{C_0} \times 100 \quad (3)$$

3. Results and discussion

3.1. Optimization of AA concentration

The AA concentration for synthesis of suitable AA hydrogel was optimized for a fixed adsorbed dose of 30 kGy. In the concentration range 5–10%, a highly viscous but flowing solution was obtained. On the other hand, for AA concentrations in the range of 20–50%,

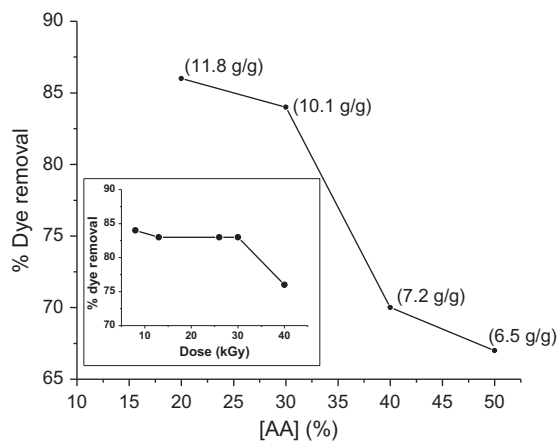


Fig. 2. Dye removal by AA hydrogel prepared (Dose = 30 kGy) from different AA concentration. Inset: Dye removal by AA ([AA] = 20% (w/v)) hydrogel prepared at different absorbed dose.

gels with good strength and different extent of swelling were formed. Fig. 2 shows the dye (BR 29) uptake capacity of hydrogel prepared with varying AA concentrations. It is clear from the figure that hydrogel synthesized from 20% AA showed maximum dye uptake and at higher AA concentration the dye uptake decreased. The water uptake for different hydrogels was studied to probe this observation. The equilibrium water uptake for the gels is shown in the brackets in Fig. 2. It clearly shows maximum water uptake for 20% AA hydrogel followed by a decrease with increasing AA concentration. The swelling behaviour of radiation-synthesized AA hydrogel with AA concentration >50% has been reported earlier, where it has been clearly mentioned that these AA hydrogel swell in three steps of initial fast swelling followed by a long phase of extremely low swelling and final step of spurt in swelling before reaching equilibrium [20]. The second step of swelling is so slow that it takes about three months for gels to reach equilibrium swelling. Thus, either for >20% AA hydrogel, the equilibrium swelling was not attained or the gels formed with >20% AA were more crosslinked. It has also been reported that crosslink density (extent of crosslinking) is a function of monomer/polymer concentration [21,22]. It seems for the studied system at an absorbed radiation dose the crosslinking density was much higher for gels synthesized at higher monomer concentration which is also reflected in lower equilibrium water uptake. The lower water uptake would obviously result in lower dye uptake as observed in the study. Therefore, further studies were carried out at 20% AA concentration.

3.2. Optimization of adsorbed dose

The optimum absorbed dose for the synthesis of 20% AA hydrogel is shown in the inset of Fig. 2. It shows that dye (BR 29) removal capacity of AA hydrogel remained almost constant up to 30 kGy and decreased at higher doses. This observation suggests that although the crosslinking density of the AA hydrogel is supposed to increase with dose [23], but it did not have any significant effect on the extent of dye uptake capacity up to 30 kGy. The effect was pronounced at >30 kGy dose which led to the decrease in dye uptake. Therefore, 20% AA concentration and 30 kGy dose were optimized to prepare the hydrogel for further studies.

3.3. Effect of pH on dye removal capacity of AA hydrogel

The effect of solution pH on the removal of BR 29 and MB dyes by AA hydrogel is shown in Fig. 3. The

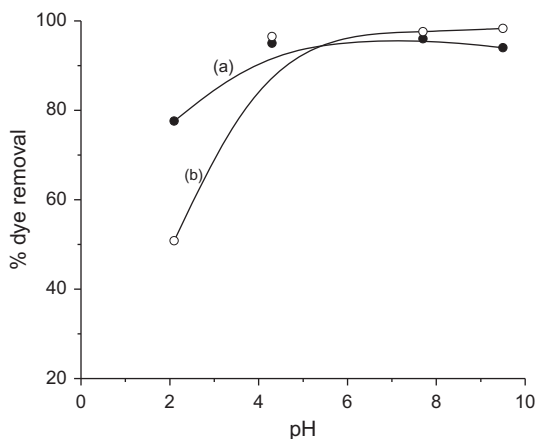


Fig. 3. Effect of pH on dye adsorption by AA hydrogel (a) BR 29 and (b) MB.

dye removal capacity for both the dyes by AA hydrogel increased with pH and reached a plateau in the pH range of 4–10 (~97%). At acidic pH (pH ~2), the acrylic acid exists in non-ionic protonated ($pK_a \sim 4.3$) form. As a result, there is feeble negative charge on AA hydrogel to electrostatically bind the basic dyes BR 29 or MB resulting in lower dye uptake. The difference in the extent of dye removal capacity by AA hydrogel for BR 29 and MB dyes at pH ~2 indicates that mode of interaction of the two dyes with AA hydrogel is different. The lower extent of removal of MB dye (~51%) compared with BR 29 (~81%) at pH ~2 (when gel is protonated) indicates that MB predominantly interacts with gel through ionic interaction. The gel is feebly ionized at pH ~2 resulting into lower extent of MB uptake. On the other hand, the extent of fully deprotonated (i.e. ionized) AA increases at higher pH. Then, the availability of negative charge on the gel and electrostatic repulsion between the charges on the gel enhances the kinetics of dye uptake.

3.4. Equilibrium adsorption on AA hydrogel

Equilibrium adsorption isotherms correlate the amount of adsorbate in the liquid phase and adsorbed on the surface of the adsorbent at equilibrium at constant temperature. Two well-known adsorption isotherms, Langmuir and Freundlich models were applied to describe the adsorption phenomenon at solid–liquid interface [24]. Langmuir adsorption isotherm assumes monolayer adsorption of adsorbate over a homogeneous adsorbent surface with finite number of identical and equivalent sites with no lateral interaction and steric hindrance between the adsorbed molecules [25]. The mathematical expression of the Langmuir model is given by following Eq. (4):

$$q_e = \frac{q_{\max} b C_e}{(1 + b C_e)} \quad (4)$$

where q_e is the solid-phase dye concentration at equilibrium (in mg/g), C_e is the liquid-phase dye concentration at equilibrium (in mg/L), q_{\max} is the maximum adsorption capacity of the adsorbent (in mg/g) assuming monolayer coverage by the adsorbate and b is a Langmuir adsorption constant (in L/mg). The Langmuir equation can be described in the linearized form as Eq. (5):

$$\frac{C_e}{q_e} = \frac{1}{q_{\max} b} + \frac{C_e}{q_{\max}} \quad (5)$$

The linear plot of C_e/q_e vs. C_e gives a straight line with slope of $(1/q_{\max})$ and intercept of $(1/q_{\max} b)$ and from the slope and intercept, theoretical monolayer adsorption capacity q_{\max} can be evaluated. Fig. 4 and its inset represent the linear and equilibrium Langmuir isotherms for the adsorption of two dyes BR 29 and MB at room temperature, respectively. q_{\max} and b were determined from the slope and intercept of the Fig. 4 and are presented in Table 1. It shows that higher q_{\max} value was obtained for the adsorption of BR 29 (1,123 mg/g or 3.04 mmol/g) than MB (220 mg/g or 0.69 mmol/g). Though both dyes are in monovalent state in aqueous medium, still the extent of uptake was different. It has been well documented that extent of dye adsorption is not solely because of electrostatic interaction in such adsorbent–adsorbate system. Several other factors, such as size of dye molecule, hydrophobic interaction of dye with polymer backbone, self-association property of dye and number of anionic sites which surround dye molecule influence the adsorbent–adsorbate interaction [26–30]. It is clear that all these combined effects result in much better interaction of BR 29 with AA hydrogel. However, the adsorption capacity for both dyes was found to be superior than that reported for activated carbon prepared from *Euphorbia antiquorum* L wood [31], *Delonix regia* Pods [32] and hydrolyzed wheat straw [33]. The adsorption capacity of the optimized AA hydrogel showed superior adsorption capacity than a few other hydrogels [9–14].

The essential characteristics of the Langmuir isotherm can be expressed by a dimensionless constant, R_L , that is given by Eq. (6) [25]

$$R_L = \frac{1}{(1 + b C_0)} \quad (6)$$

where C_0 is the adsorbate initial concentration (in mg/L). The value of R_L indicates the nature of adsorption process.

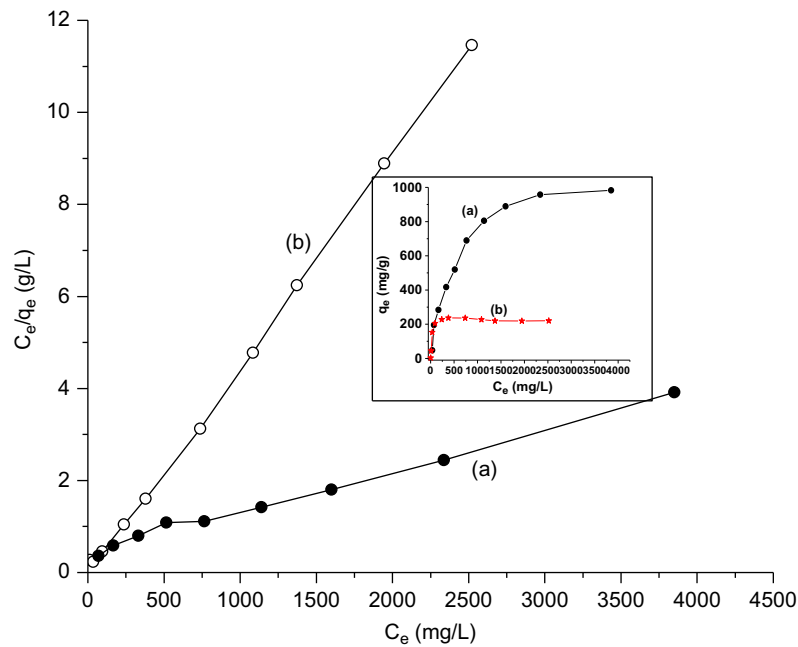


Fig. 4. Langmuir adsorption isotherms for dye adsorption on AA hydrogel (a) BR 29 and (b) MB. Inset: Equilibrium adsorption isotherm for dye adsorption on AA hydrogel (a) BR 29 and (b) MB.

Table 1

Langmuir and Freundlich adsorption parameters for adsorption of BR 29 and MB dyes onto AA hydrogel adsorbent

Langmuir					
Dye	q_{\max} (mg/g)	q_{\max} (mmol/g)	q_{exp} (mmol/g)	b (L/mg)	R^2
BR 29	1,123	3.04	2.67	2.0×10^{-3}	0.991
MB	220	0.69	0.69	14.29	0.998
Freundlich					
Dye	K_F	n	R^2		
BR 29	11.4	1.7	0.881		
MB	10.08	2.1	0.696		

R_L values calculated were in the range of $0.10 < R_L < 0.98$ and $2.5 \times 10^{-5} < R_L < 0.01$ in the concentration range of 10–5,000 mg/L for BR 29 and MB dyes, respectively. R_L values for adsorption of both the dyes lie in between 0 and 1 indicating favourable adsorption of these dyes onto AA hydrogel.

The Freundlich adsorption isotherm assumes multilayer adsorption on heterogeneous surfaces with interaction between the adsorbed molecules [34]. The Freundlich equation is expressed by Eq. (7)

$$q_e = K_F C_e^{\frac{1}{n}} \quad (7)$$

where q_e is the solid-phase dye concentration at equilibrium (in mg/g), C_e is the liquid-phase dye

concentration at equilibrium (in mg/L), K_F (in $\text{mg g}^{-1} \text{L}^{-1/n} \text{mg}^{1/n}$) and n are Freundlich isotherm constant and heterogeneity factor and have been used to describe adsorption capacity and intensity, respectively [34]. To determine the constants K_F and n , the Freundlich equation is expressed in the linearized form (Eq. (8)).

$$\ln q_e = \ln K_F + \frac{1}{n} \ln C_e \quad (8)$$

The equilibrium adsorption data for BR 29 and MB were plotted by fitting in the model Eq. (8) and the profiles are shown in Fig. 5. The K_F and n values were determined from the intercept and the slope of the profiles, respectively, and are shown in Table 1.

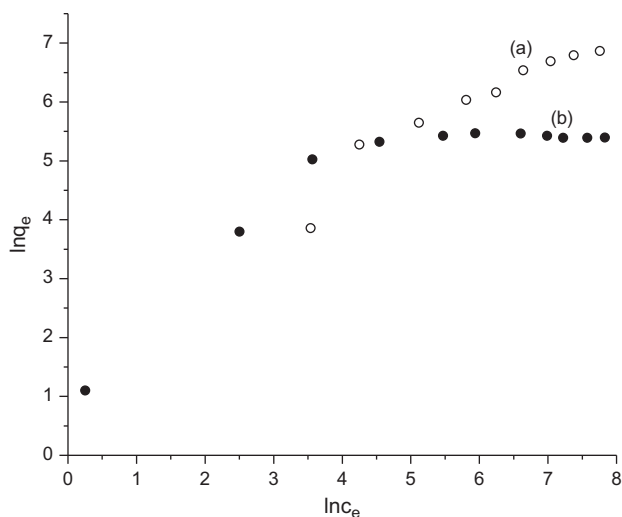


Fig. 5. Freundlich adsorption isotherms for dye adsorption on AA hydrogel (a) BR 29 and (b) MB.

However, to choose better fitting model, regression coefficient (R^2) was used as criteria [35]. The higher R^2 values for Langumir model (~ 0.991 for BR 29 and 0.998 for MB) compared with Freundlich isotherm (0.881 for BR 29 and 0.696 for MB) and better degree of agreement between q_{exp} and q_{max} predicted from Langmuir isotherm model for adsorption of BR 29 and MB onto AA hydrogel suggested that adsorptions of both of these dyes are better described by the Langmuir model over the whole concentration range studied.

The equilibrium adsorption of BR 29 and MB by both dry and wet gels was studied to understand the role of the physical state of the ionic gel in the adsorption process. The results are shown in Table 2. The relative uptakes of both the dyes were decreased when the wet gel was used for the removal of dye from its

Table 2
The relative uptake of water and dye molecules by different state of gels (in wt%)

	Dry gel dipped in water		Dry gel dipped in 500 ppm aqueous dye solution		Dry gel swelled in water initially and then dipped in 500 ppm aqueous dye solution	
	H ₂ O	Dye	H ₂ O	Dye	H ₂ O	Dye
BR 29	100	0	96	4	98.2	1.8
MB	100	0	97	3	99.6	0.4

aqueous solution. This is attributed to the change in the electrostatic osmotic pressure (π_{el}) in dry-unswelled and wet-swelled hydrogels. The π_{el} is defined as following Eq. (9):

$$\pi_{el} = k_B T \rho(r, \Phi) \tag{9}$$

where k_B is the Boltzman constant, T is the temperature in absolute scale and $\rho(r, \Phi)$ is the concentration number density of ionic charge inside the hydrogel and Φ is the ionic potential experienced by an ion in solution at a distance r from the charge centre inside the hydrogel. The Φ value is comparatively lower in the wet gel than dry gel as the charge centres in wet AA hydrogel are screened by the solvation layer of water molecules. As a result, $\rho(r, \Phi)$ as well as π_{el} are greater in dry gel as compared with wet gel. This is the driving force behind the higher extent of dye uptake by the dry gel. The difference in the extent of dye uptake by wet and dry hydrogels is very insignificant, because the electrostatic osmotic pressure effect is very trivial comparative to the other osmotic pressure components acting on water uptake and swelling of hydrogels.

3.5. Adsorption kinetics

Adsorption kinetics is one of the most important parameter which governs the solute uptake rate. It represents adsorption efficiency of adsorbent for design operation and optimization and provides valuable information on the mechanism of the adsorption process [36]. The pseudo-first-order [37] and pseudo-second-order kinetic models [38] were used to determine the kinetics of dye adsorption onto AA hydrogel adsorbent.

3.5.1. Pseudo-first-order kinetic model

A simple kinetic analysis of adsorption is expressed by pseudo-first-order equation (also known as Lagergren equation) as shown in the Eq. (10):

$$\frac{dq_t}{dt} = k_1 (q_e - q_t) \tag{10}$$

where q_t and q_e are the adsorption capacity at time t and at equilibrium (in $mg\ g^{-1}$), k_1 is the pseudo-first-order rate constant (in h^{-1}) and t is the adsorption time (in h). The integration of Eq. (10) for boundary condition, $q_t = 0$ at $t = 0$ and $q_t = q_t$ at $t = t$ leads to Eq. (11):

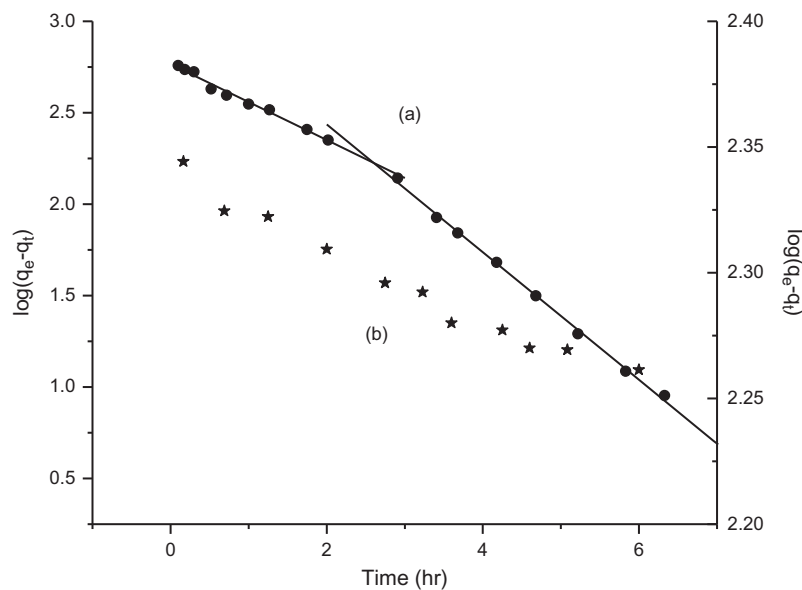


Fig. 6. Pseudo-first-order adsorption kinetics onto AA hydrogel (a) BR 29 (Left y-axis) and (b) MB (Right y-axis).

$$\log (q_e - q_t) = \log q_e - \frac{k_1 t}{2.303} \quad (11)$$

The slope and intercept of the linear plot of $\log (q_e - q_t)$ vs. t were used to estimate k_1 and $q_{e,cal}$ respectively. Fig. 6 shows pseudo-first-order plot for the adsorption of BR 29 and MB onto AA hydrogel. The k_1 and $q_{e,cal}$ determined from the plot for the adsorption of two dyes are listed in Table 3 along with the corresponding R^2 values. From Fig. 6, it is clear that BR 29 adsorption onto AA hydrogel has two different k_1 values for two different time scales ranging 0.1–2.0 and 2.9–7.2 h. It was found that the $q_{e,cal}$ value was not in good agreement with the $q_{e,exp}$ value at higher time scale (2.9–7.2 h). Therefore, it can be concluded that the pseudo-first-order model for the adsorption of BR 29 onto AA hydrogel fits well only in initial times (0.1–2.0 h). Similar observations for dye adsorption

have been reported earlier for other systems by Ho and McKay where they reported pseudo-first-order model is applicable for initial stage of the adsorption process [39]. On the other hand, based on the kinetic parameters obtained for adsorption of MB onto AA hydrogel (shown in Table 3), it can be concluded that its adsorption does not follow pseudo-first-order kinetic model.

3.5.2. Pseudo-second-order kinetic model

The differential expression of the pseudo-second-order model is given as Eq. (12)

$$\frac{dq_t}{dt} = k_2 (q_e - q_t)^2 \quad (12)$$

Integrating Eq. (12) and rearranging it gives rise to a linear expression of the pseudo-second-order model

Table 3
Kinetic parameters for adsorption of BR 29 and MB dyes onto AA hydrogel adsorbent

Pseudo-first order kinetic model							
Dye	K_1 (h^{-1})		R^2	$q_{e,exp}$ (mg/g)		$q_{e,cal}$ (mg/g)	
BR 29	0.478 (0.1–2.0 h)	0.8034 (2.9–7.2 h)	0.985 (0.1–2.0 h) 0.998 (2.9–7.2 h)	550	583 (0.1–2.0 h)	1,088 (2.9–7.2 h)	
MB	0.032		0.963	80	219		
Pseudo-second order kinetic model							
Dye	K_2 ($h^{-1} g mg^{-1}$)		R^2	$q_{e,exp}$ (mg/g)		$q_{e,cal}$ (mg/g)	
BR 29	6.4×10^{-4}		0.988	550	769		
MB	3.5×10^{-3}		0.997	80	74		

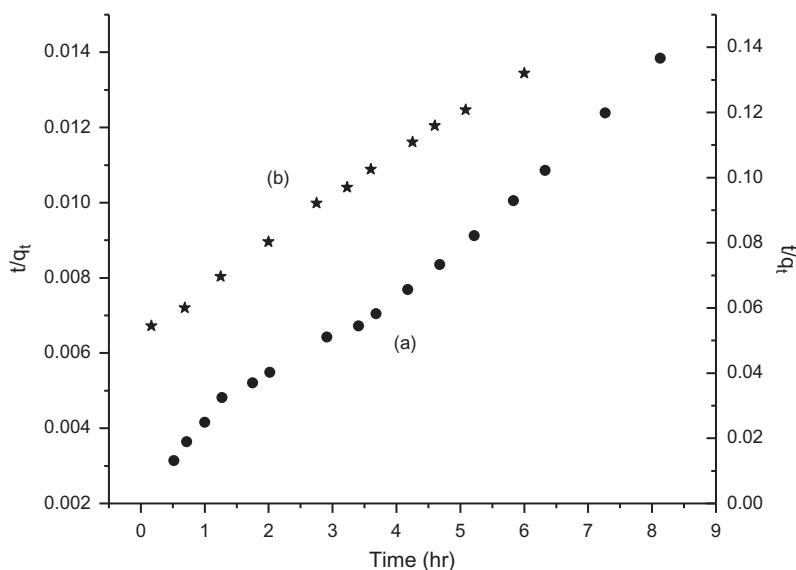


Fig. 7. Pseudo-second-order adsorption kinetics onto AA hydrogel (a) BR 29 (Left y-axis) and (b) MB (Right y-axis).

given as Eq. (13), which is mostly used for solid–liquid adsorption systems.

$$\frac{t}{q_t} = \frac{1}{k_2 q_e^2} + \frac{t}{q_e} \quad (13)$$

where k_2 is the pseudo-second-order adsorption rate constant (in $\text{g mg}^{-1} \text{h}^{-1}$) and other parameters are same as described in pseudo-first-order kinetic model. Fig. 7 shows t/q_t vs. t plot for the adsorption of BR 29 and MB onto AA hydrogel. Predicted equilibrium adsorption amount $q_{e,cal}$ and k_2 were calculated from the slope and intercept of the linear plot for BR 29 and MB, respectively, and are shown in the Table 2. Unlike pseudo-first-order model, the pseudo-second order model is more likely to predict the behaviour over the entire range of the adsorption process [40]. The high R^2 and good agreement between the $q_{e,cal}$ and $q_{e,exp}$ values indicate that the MB adsorption on AA hydrogel system follows pseudo-second order kinetics. Similar phenomena were observed in the adsorption of MB onto activated carbon [41]. On the other hand, low R^2 and poor agreement between the $q_{e,cal}$ and $q_{e,exp}$ values for BR 29 adsorption on AA hydrogel indicates BR 29 adsorption does not follow pseudo-second-order kinetics.

3.6. Desorption study

The regeneration of the adsorbent by desorption of adsorbed dyes in a suitable eluent is prerequisite for the success of the adsorption process. Thus, desorption of dyes was studied in some solvents or

solutions in which desorption was expected, and the results are shown in Fig. 8. Desorption of MB was less in methanol and urea solution which are known to disrupt hydrophobic interaction [42,43] where as its desorption was significantly high in 1 N HCl which is expected to disrupt ionic interaction. However, the extent of desorption of BR 29 was almost similar in 1 N HCl as well as in methanol and urea solution. This indicated that adsorption of dyes on to adsorbent was not solely due to ionic interaction but might be due to cumulative effect of many attractive forces *viz.* ionic interactions, hydrophobic interactions, van der waals forces, hydrogen bonding, etc. [44].

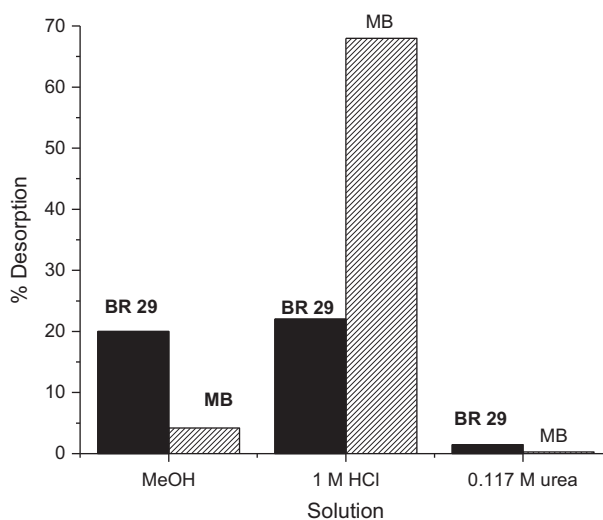


Fig. 8. Desorption of dyes in different solutions.

Thus, it could be fairly said that MB is adsorbed predominantly through ionic interaction, whereas BR 29 adsorption on to AA hydrogel follows ionic as well as hydrophobic interactions.

4. Conclusion

Gamma radiation synthesized AA hydrogel adsorbent showed superior uptake of BR 29 and MB from aqueous solution compared with the activated carbon and a few other hydrogels. The optimized AA hydrogel was efficient to adsorb dye from its aqueous solution in a wide range of concentration (10–5,000 mg/L). The extent of dye uptake was strongly depended on concentration of the monomer initially taken for gel formation and on the dose imparted. Equilibrium adsorption of both the dyes BR 29 and MB were better described by Langmuir adsorption model. The adsorption of BR 29 onto AA hydrogel follows pseudo-first-order kinetics only in the initial time scale, whereas the MB adsorption on AA hydrogel system follows pseudo-second-order kinetic model over the entire range of adsorption process. From the pH effect on the dye uptake and the desorption studies at different solvent or solutions, it can be concluded that MB is adsorbed predominantly through ionic interaction, whereas BR 29 adsorption on to AA hydrogel follows ionic and as well as hydrophobic interaction.

References

- [1] Z. Aksu, Application of biosorption for the removal of organic pollutants: A review, *Process Biochem.* 40 (2005) 997–1026.
- [2] P. Kumar, R. Agnihotri, K.L. Wasewar, H. Uslu, C.K. Yoo, Status of adsorptive removal of dye from textile industry effluent, *Desalin. Water Treat.* 50 (2012) 226–244.
- [3] J. Paul, D.B. Naik, S. Sabharwal, High energy induced decolouration and mineralization of reactive red 120 dye in aqueous solution: A steady state and pulse radiolysis study, *Radiat. Phys. Chem.* 79 (2010) 770–776.
- [4] J. Paul, A.A. Kadam, S.P. Govindwar, P. Kumar, L. Varshney, An insight into the influence of low dose irradiation pretreatment on the microbial decolouration and degradation of Reactive Red-120 dye, *Chemosphere* 90 (2013) 1348–1358.
- [5] E. Al, G. Guclu, T.B. Iyim, S. Emik, S. Ozgumus, Synthesis and properties of starch-graft-acrylic acid/nanotmorillonite superabsorbent nanocomposite hydrogels, *J. Appl. Polym. Sci.* 109 (2008) 16–22.
- [6] A.Z. Bouyakoub, S. Kacha, B. Lartiges, S. Bellebia, Z. Derriche, Treatment of reactive dye solutions by physicochemical combined process, *Desalin. Water Treat.* 12 (2009) 202–209.
- [7] K.Y. Foo, B.H. Hameed, An overview of dye removal via activated carbon adsorption process, *Desalin. Water Treat.* 19 (2010) 255–274.
- [8] G. Cole, M.K. Gok, G. Guclu, Removal of basic dye from aqueous solutions using a novel nanocomposite hydrogel N-vinyl 2-pyrrolidone/itaconic acid/organo clay, *Water Air Soil Pollut.* 224 (2013) 1760.
- [9] G.A. Mahmoud, S.E. Abdel-Aal, N.A. Badway, S.A. Abo Farha, E.A. Alshafei, Radiation synthesis and characterization of starch-based hydrogels for removal of acid dye, *Starch* 66 (2014) 400–408.
- [10] N.C. Dafader, A. Tahmina, M.E. Haque, S.P. Swapna, I. Sadia, D. Huq, Effect of acrylic acid on the properties of polyvinylpyrrolidone hydrogel prepared by the application of gamma radiation, *Afr. J. Biotechnol.* 11 (2012) 13049–13057.
- [11] M. Zendehelel, A. Barati, H. Alikhani, A. Hekmat, Removal of methylene blue dye from wastewater by adsorption onto semi-impenetrating polymer network hydrogels composed of acrylamide and acrylic acid copolymer and polyvinyl alcohol, *Iran. J. Environ. Health. Sci. Eng.* 7 (2010) 423–428.
- [12] S.R. Shirsath, A.P. Patil, R. Patil, J.B. Naik, P.R. Gogate, S.H. Sonawane, Removal of brilliant green from wastewater using conventional and ultrasonically prepared poly(acrylic acid) hydrogel loaded with kaolin clay: A comparative study, *Ultrason. Sonochem.* 20 (2013) 914–923.
- [13] L. Aberkane-Mechebbek, S.F. Larbi-Youcef, M. Mahlous, Adsorption of dyes and metal ions by acrylamide—Co—acrylic acid hydrogels synthesized by gamma radiation, *Mater. Sci. Forum* 609 (2009) 255–259.
- [14] S. Li, X. Liu, T. Zou, W. Xiao, Removal of cationic dye from aqueous solution by a macroporous hydrophobically modified poly(acrylic acid-acrylamide) hydrogel with enhanced swelling and adsorption properties, *Clean Soil Air Water* 38 (2010) 378–386.
- [15] A.A. Asem, M.D. Ahmed, A.H. Rashad, T.R. Rama, Swelling and metal ion uptake characteristics of kaolinite containing poly [(acrylic acid)-co-acrylamide] hydrogels, *Desalin. Water Treat.* 3 (2009) 73–82.
- [16] A. Pourjavadi, R. Soleyman, G.R. Bardajee, F. Seidi, γ -irradiation synthesis of a smart hydrogel: Optimization using taguchi method and investigation of its swelling behavior, *Trans. C: Chem. Chem. Eng.* 17 (2010) 15–23.
- [17] A.G.S. Prado, J.D. Torres, E.A. Faria, S.C.L. Dias, Comparative adsorption studies of indigo carmine dye on chitin and chitosan, *J. Colloid. Interface Sci.* 277 (2004) 43–47.
- [18] E. Karadag, O.B. Uzum, D. Saraydin, Swelling equilibria and dye adsorption studies of chemically cross-linked superabsorbent acrylamide/maleic acid hydrogels, *Eur. Polym. J.* 38 (2002) 2133–2141.
- [19] G.A. Mahmoud, S.E. Abdel-Aal, N.A. Badway, S.A.A. Farha, E.A. Alshafei, Radiation synthesis and characterization of starch-based hydrogels for removal of acid dye, *Starch* 66 (2014) 400–408.
- [20] Y.K. Bhardwaj, S. Sabharwal, A.B. Majali, Dynamic swelling kinetics of radiation polymerised poly(2-Hydroxy ethyl methacrylate) and 2-hydroxy ethyl methacrylate-co-ionic hydrogels-Part I: Swelling in aqueous solution, *J. Polym. Mater.* 17 (2000) 239–252.
- [21] M.Y. Kizilay, O. Okay, Effect of initial monomer concentration on spatial inhomogeneity in poly(acrylamide) gels, *Macromolecules* 36 (2003) 6856–6862.

- [22] R. Vera-Graziano, F. Hernandez-Sanchez, J.V. Cauich-Rodriguez, Study of crosslinking density in polydimethylsiloxane networks by DSC, *J. Appl. Polym. Sci.* 55 (1995) 1317–1327.
- [23] R.J. Woods, A.K. Pikaev, *Applied Radiation Chemistry: Radiation Processing*, Wiley, New York, NY, 1994, pp. 340–365.
- [24] Y.-S. Ho, R. Malarvizhi, N. Sulochana, Equilibrium isotherm studies of methylene blue adsorption onto activated carbon prepared from *Delonix regia* Pods, *J. Environ. Protect. Sci.* 32 (2009) 111–116.
- [25] I. Langmuir, The constitution and fundamental properties of solids and liquids. Part I. Solids, *J. Am. Chem. Soc.* 38 (1916) 2221–2295.
- [26] F. Ismail, M. Schoenleber, R. Mansour, B. Bastani, P. Fieldena, N.J. Goddarda, Strength of interactions between immobilized dye molecules and sol-gel matrices, *Analyst* 136 (2011) 807–815.
- [27] W. Zhijian, J. Hyeonwoo, L. Kangtaek, Kinetics and thermodynamics of the organic dye adsorption on the mesoporous hybrid xerogel, *Chem. Eng. J.* 112 (2005) 227–236.
- [28] M.S. Chiou, H.Y. Li, Adsorption behavior of reactive dye in aqueous solution on chemical cross-linked chitosan beads, *Chemosphere* 50 (2003) 1095–1105.
- [29] J. Wang, P. Somasundaran, D.R. Nagaraj, Adsorption mechanism of guar gum at solid-liquid interfaces, *Miner. Eng.* 18 (2005) 77–81.
- [30] R. Blackburn, Natural polysaccharides and their interactions with dye molecules: Applications in effluent treatment, *Environ. Sci. Technol.* 38 (2004) 4905–4909.
- [31] P. Sivakumar, P.N. Palanisamy, Adsorption studies of Basic Red 29 by a non-conventional activated carbon prepared from *Euphorbia antiquorum* L, *Int. J. Chem. Tech. Res.* 1 (2009) 502–510.
- [32] Y.-S. Ho, R. Malarvizhi, N. Sulochana, Equilibrium isotherm studies of methylene blue adsorption onto activated carbon prepared from *Delonix regia* Pods, *J. Environ. Protect. Sci.* 3 (2009) 111–116.
- [33] F. Batzias, D. Sidiras, E. Schroeder, C. Weber, Simulation of dye adsorption on hydrolyzed wheat straw in batch and fixed-bed systems, *Chem. Eng. J.* 148 (2009) 459–472.
- [34] H.M.F. Freundlich, Über die adsorption in lösungen (Over the adsorption in solutions), *Zeitschrift für Physikalische Chemie (Leipzig)* (Journal of Physical Chemistry (Leipzig)) 57A (1906) 385–470.
- [35] O. Tunc, H. Tanaci, Z. Aksu, Potential use of cotton plant wastes for the removal of Remazol Black B Reactive dye, *J. Hazard. Mater.* 163 (2009) 187–198.
- [36] R.E. Treyball, *Mass Transfer Operations*, third ed., McGraw Hill, New York, NY, 1980.
- [37] M.S. Chiou, H.Y. Li, Adsorption behavior of reactive dye in aqueous solution on chemical cross-linked chitosan beads, *Chemosphere* 50 (2003) 1095–1105.
- [38] L. Semerjian, Equilibrium and kinetics of cadmium adsorption from aqueous solutions using untreated *Pinus halepensis* sawdust, *J. Hazard. Mater.* 173 (2010) 236–242.
- [39] Y.S. Ho, G. McKay, Pseudo-second order model for sorption processes, *Process Biochem.* 34 (1999) 451–465.
- [40] C. Namasivayam, D. Kavitha, Removal of Congo red from water by adsorption onto activated carbon prepared from coir pith, an agricultural solid waste, *Dyes Pigm.* 54 (2002) 47–58.
- [41] A. Gurses, C. Dogar, S. Karaca, A.C. Ikyildiz, M.R. Bayrak, Production of granular activated carbon from waste *Rosa canina* sp. seeds and its adsorption characteristics for dye, *J. Hazard. Mater.* 131 (2006) 254–259.
- [42] C.H. Liu, J.S. Wu, H.C. Chiu, S.Y. Suen, K.H. Chu, Removal of anionic reactive dyes from water using anion exchange membranes as adsorbers, *Water. Res.* 41 (2007) 1491.
- [43] Y.K. Bhardwaj, S. Sabharwal, A.B. Majali, Sorption kinetics of radiation polymerized poly(2-hydroxyethyl methacrylate and 2-hydroxyethylmethacrylate-co-n-vinyl pyrrolidone hydrogels, *J. Poly. Mater.* 11 (1994) 29–34.
- [44] W. Zhijian, J. Hyeonwoo, L. Kangtaek, Kinetics and thermodynamics of the organic dye adsorption on the mesoporous hybrid xerogel, *J. Chem. Eng.* 112 (2005) 227.